

# Modelling and Analysis of Electric Vehicle DC Fast Charging Infrastructure Based on PSIM

Agus Purwadi<sup>1</sup>, Nadhilah Shani, Nana Heryana  
School of Electrical Engineering and Informatics  
Institut Teknologi Bandung  
Bandung 40132 Indonesia  
<sup>1</sup>apurwadi57@gmail.com

Tri Hardimasyar<sup>2</sup>, M.Firmansyah, Arrester SR  
Centre of Research and Development  
PT. PLN (Persero)  
Jakarta 12760, Indonesia  
<sup>2</sup>masdede@gmail.com

**Abstract**—In this paper, DC fast charging infrastructure model using PSIM is proposed. DC Fast charging infrastructure is modelled as a bidirectional three-phase PWM rectifier with constant output voltage control and unity power factor input current control. The specification of the DC fast charging infrastructure is a constant voltage charging mode with capacity of 50 kW. Using a proposed model, a simulation on various levels of State Of Charge (SOC) which are simplified to the battery voltage droplevels was also performed. Lithium ion batteries was used and modelled by Thevenin equivalent battery model. Analysis of the DC fast charging impacts to the grid seen from the input current Total Harmonics Distortion (THD) were conducted.

**Keyword** : Three phase bidirectional PWM rectifier; constant voltage charging; THD; DC Fast charging infrastructure; PSIM

## I. INTRODUCTION

Mobility is one of the basic needs of human being. Development in technologies and faster delivery of information trigger the human need of higher mobility from one place to another. So, the growth of transportation needed by human also increases significantly. Environmental issues about carbon emission as a result of engine combustion are indicated as one of the main cause of global warming. Besides that, increasing of the Internal Combustion Engine (ICE) cars threatened our fossil fuel that is considered as non-renewable energy. Transition from ICE cars to electric cars is an alternative to solve those problems.

Electric cars is better than ICE vehicle because its higher efficiency in energy consumption and no carbon emission that produced by electric cars [1]. Electric cars also have main components to support them to run well, they are battery and its charger. There are two kind of charger, on-board charger and off-board charger. On-board charger is a slow charger (6-18 hours) that is built-in with the car while off-board charger is fast charger (10-30 minutes) that similar with gas station for ICE cars [1], [3]. On board charger is limited only for level 1 due to weight, dimension, and price [4]. Off board charger is faster than on board charger but it has limited flexibility for charging battery in various places [6].

Challenges faced in the development of electric car are on mileage and charging time that limiting performance of electric car [2]. In the future time when electric cars are a common use, off-board charger that can charge battery in short time will be highly needed. This off-board charger needs high input power that can affect the grid. Loading of this fast charger need to be regulated and watched closely. So a further study about this fast charger must be done. Modelling of fast charger will be very useful for analyzing the effect of fast charging to the grid before implementation. Modelling will be made in PSIM simulation software version 9.0 ( a simulation software designed for power electronics, motor control and dynamic system simulation) and simulate in the various value of battery SOC. In this paper, modelling of fast charger will be explain in section II, simulation and analysis in section III, and conclusion in section IV.

## II. DC FAST CHARGER MODELING USING PSIM

Proposed model of fast charger is a model of each component of typical charger that is commonly used. Modelling starts from input AC source until the load, which is battery. This picture represents the model of fast charger that is proposed.

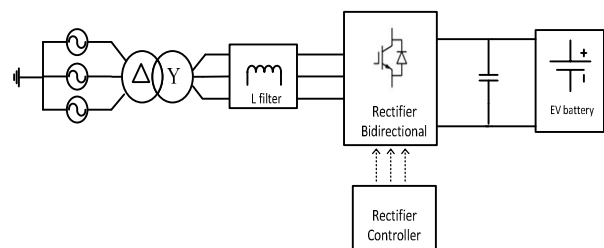


Figure 2.1 Electric Car DC fast charger model

Modelling is done from AC source side 20 kV that is step downed into 380 V AC by delta- wye transformer. Then, output of this transformer goes into L filter, then become input for controlled bidirectional rectifier. This modelling needs some controls, with L filter the current control only needs PI controller [7]. The output of this bidirectional rectifier is constant DC voltage

The DC current charge the capacitor, then the current from the capacitor will flow into the battery. Modelling is made as a constant voltage mode while charging. Rectifier that is used as modelling is a rectifier that can work in two quadrants. This type of rectifier was chosen as a model because it can drain power from the source to the load side or from the side of the load to the source. So the rectifier is working in two modes, namely rectifier mode and inverter mode.

Bi-directional rectifier is modelled with three-phase PWM rectifier using IGBT switches. PWM turns the switch on and off with certain fundamental template, such as sinusoidal current or voltage [8]. The mechanism of action of the rectifier is as follows.

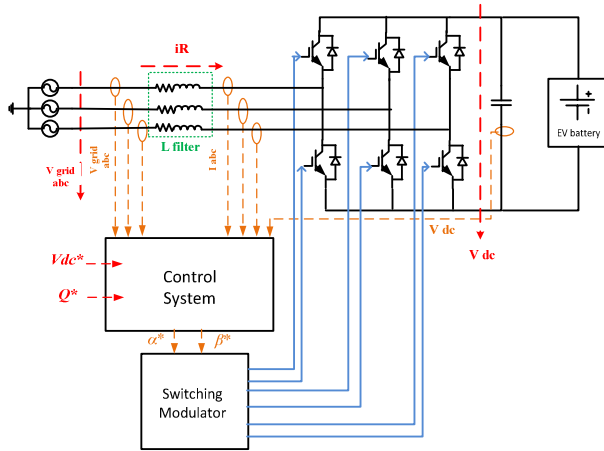


Figure 2.2 Three phase bidirectional PWM rectifier scheme

From the scheme above, it can be seen that there are two references that are used to control the system,  $V_{dc}^*$  and  $Q^*$ .  $V_{dc}^*$  will provide a reference for dc voltage at the desired nominal output in capacitor. While  $Q^*$  is proportional to the reference of q-axis current ( $i_q^*$ ) that will determine how reactive power absorbed by the rectifier. By adjusting the q-axis, then the PF (power factor) can be arranged as well. Grid voltages  $v_a$ ,  $v_b$ , and  $v_c$ , the input current,  $i_b$ ,  $i_c$ , and dc voltage  $v_{dc}$ , is used as a feedback parameter in the control system.

Grid voltages  $v_a$ ,  $v_b$ , and  $v_c$  will be used as a reference phase angle and voltage to be supplied when a rectifier is working in bidirectional power flow in inverter mode. The input current  $i_a$ ,  $i_b$ , and  $i_c$  are transformed using Park transform into  $i_d$  and  $i_q$  that would control the switching of switches. Active current  $i_d$ , will be compared with the results of the reference current  $i_d^*$  as the result of  $V_{dc}$  output control which is read every time. While current  $i_q$ , will be compared with the reference current  $i_q^*$  ( $Q^*$ ), according to the given reference.  $I_d$  and  $i_q$  currents which have controlled is converted into a voltage and transformed back into three phases. Result of the transformation is to be compared using a triangular signal as the switching signal of IGBT.

Modeling of fast charging infrastructure is at a voltage level 600 V, so the battery model as load must be adjusted. Battery load is modeled with a nominal voltage 600 V, with each cell is worth about 4 V, and arrayed in series consists of 150 cells due to the battery model specification in [9]. Battery model will be simulated at different values of the dependent VOC that represent SOC. For Lithium ion battery, voltage drop of each cell when the lowest SOC is about 23% is between 77% - 90% of nominal voltage battery.

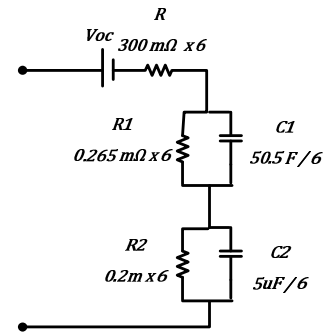


Figure 2.3 Battery model approach 600 V for 150 cells arranged series [10]

There are several kinds of control system used by bidirectional rectifier, they are angle control, input current control and the output dc voltage control. The control scheme is as follows.

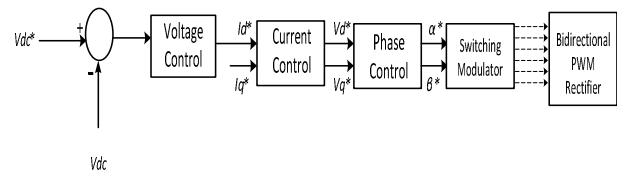


Figure 2.4 Bidirectional Rectifier PWM control scheme [11]

Phase-locked loop is needed to get the angle of reference voltage used for three phase currents and voltages transformation into dq axis in synchronous framework used in control systems. Besides that, the reference angle PLL output is needed for grid synchronization when the power flow occurs from the source to the load (inverter mode).

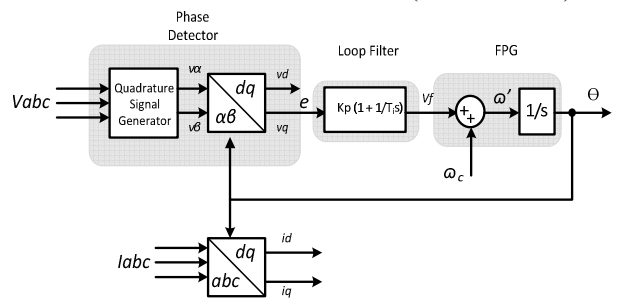


Figure 2.5 Phase Locked Loop Block Diagram and dq transformation framework

To control the AC current source and dc voltage output, the bidirectional three-phase PWM rectifier is modelled with model like the picture below.

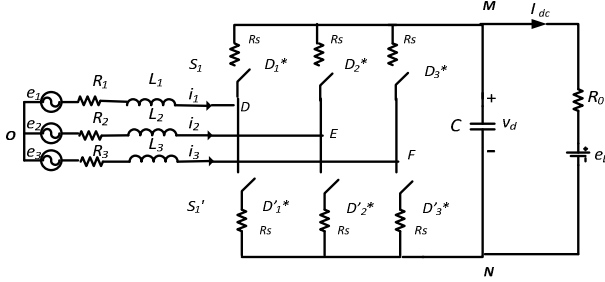


Figure 2.6 VSC circuit diagram [13]

From that figure, the mathematical equation is as follows. [13]

$$C \frac{dv_d}{dt} = \sum_{k=1}^3 i_k d_k^* - i_{dc} \quad (2.1)$$

$$L \frac{di_k}{dt} + Ri_k = e_k - v_d (d_k^* - \frac{1}{3} \sum_{k=1}^3 d_k^*) \quad (2.2)$$

where :

- $k$  phase sequence index {1,2,3}
- $d_k$  switching function
- $v_d$  dc voltage
- $i_k$  line current
- $e_k$  phase voltage
- $L$  inductance  $L$
- $R$  resistance  $R_s + R_k$

By changing the equation into dq frame, the equation becomes

$$C \frac{dv_c}{dt} = \frac{3}{2} (i_d^e d_d^e + i_q^e d_q^e) - i_{dc} \quad (2.3)$$

$$L \frac{di_d^e}{dt} + \omega L i_q^e + Ri_d^e = e_d^e - v_{dc} d_d^e \quad (2.4)$$

$$L \frac{di_q^e}{dt} - \omega L i_d^e + Ri_q^e = e_q^e - v_{dc} d_q^e \quad (2.5)$$

Because the current cannot be controlled independently, the current controller block diagram is as follows.

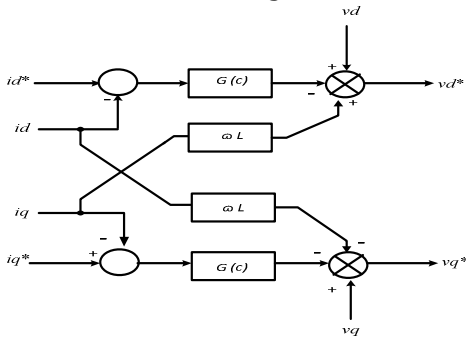


Figure 2.7 Proposed current controlled block[14]

Then the current control block diagram and control the output dc voltage is as follows.

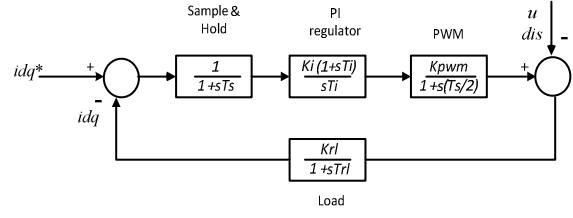


Figure 2.8 Current control loop block diagram [14]

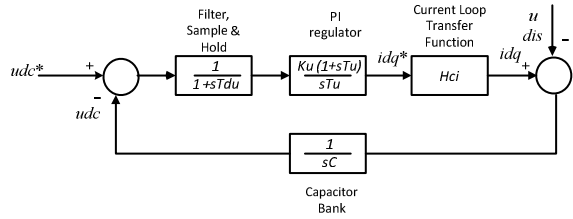


Figure 2.9 DC voltage control loop block diagram [14]

The value of gain in PI regulator depends on value of capacitor C, time constant T, and  $\alpha$  that can be seen in [12].

### III. SIMULATION RESULTS AND ANALYSIS

Simulation is performed using PSIM software 9.0. Simulations is performed with the following parameters.

TABLE 3.1 THE CIRCUIT SIMULATION PARAMETERS FOR FAST CHARGING INFRASTRUCTURE MODEL

Circuit Parameter	Value
Fast charging model capacity	50 kW
Charging voltage level	600 V dc
Source Voltage (V line-to-line) 50 Hz	380 V
Resistance R	0.12
Filter L	5 mH
Switching frequency	5 kHz
DC Link	330 uF
<b>Control System</b>	
PLL $\kappa_f$ Gain Constant	0.0707 rad/V.s
PLL $\tau_f$ Time Constant	0.0628 s
Current Control $K_i$ Gain Constant	2 A/V
Current Control $K_i$ Time Constant	10 ms
Voltage Control $K_u$ Gain Constant	0.165 V/A
Voltage Control $\tau_u$ Time Constant	5 ms
<b>Battery Model</b>	
Ohmic Resistance, R	1.8 $\Omega$
Polarization Resistance, $R_1$	1.59 m $\Omega$
Equivalent Capacity, $C_1$	8.42 F
Polarization Resistance, $R_2$	1.2 m $\Omega$
Equivalent Capacity, $C_2$	0.83 uF

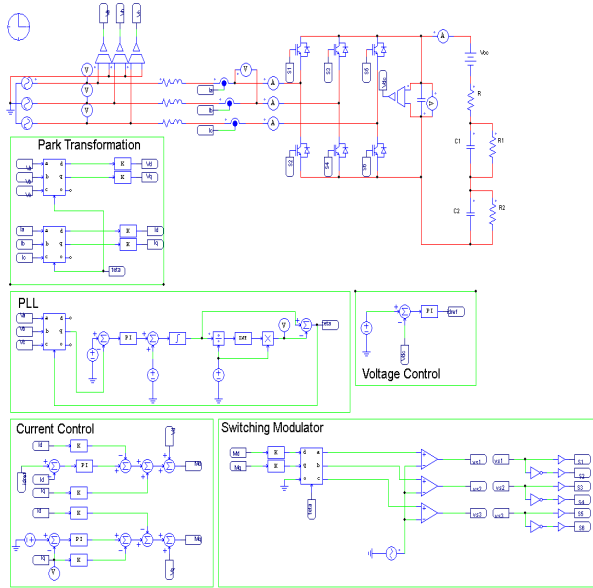


Figure 3.1 Circuit of modelled fast charger infrastructure in PSIM 9.0

Circuit model of fast charging infrastructure with its control system depicted in Figure 3.1. Simulation results for the PLL as the control angles is correct, it looks like Figure 3.2.

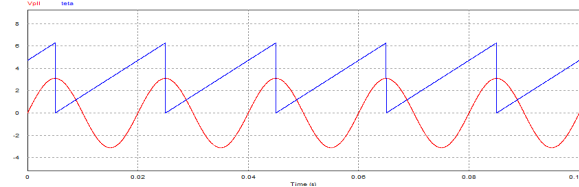


Figure 3.2 PLL Output Angle Response

Current control system has been running well visible from the  $i_q$  current is zero for reactive grid power control as shown in Figure 3.3.

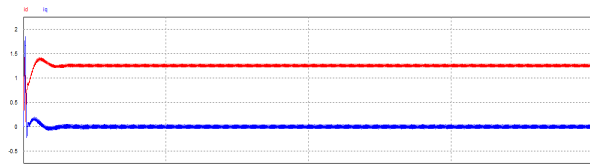


Figure 3.3 Simulation results of  $i_d$  and  $i_q$  current control response

Output dc voltage control is used to control the magnitude of the average dc voltage rectifier with the desired reference. By changing the desired reference voltage, then the modulator will arrange switches to switch the bidirectional rectifier so that the average dc voltage output will be equal to the reference value. Simulation results of the control voltage that has been working well looks like Figure 3.4 - 3.6 below.

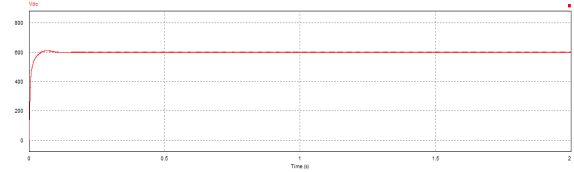


Figure 3.4 Simulation results with a control voltage 600 V as voltage reference

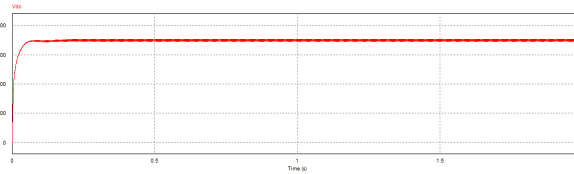


Figure 3.5 Simulation results with a control voltage 700 V as voltage reference

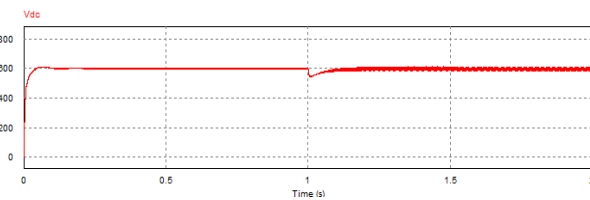


Figure 3.6 Voltage control response when load change suddenly in  $t=1s$

Fast charging infrastructure model using bidirectional three-phase PWM rectifier has the characteristic can drain power from the load back to the source. Reverse power flow simulation results can be seen from Figure 3.7. Power flow back to the source occurs when the voltage at the load is higher than the output voltage is shown by the bidirectional rectifier current  $i_{dc}$  and  $i_q$  are negative.

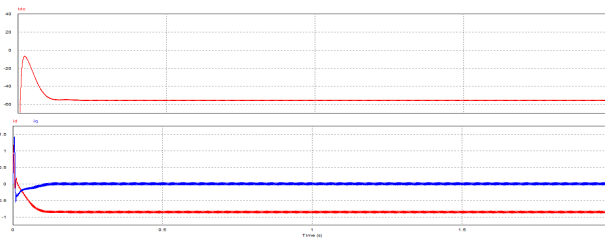
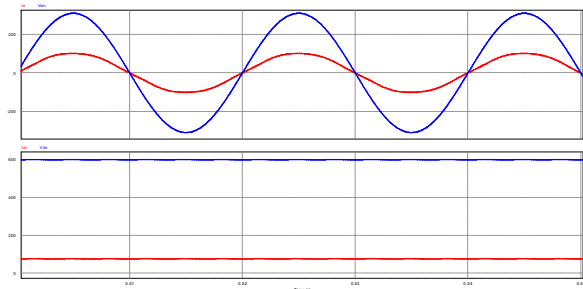
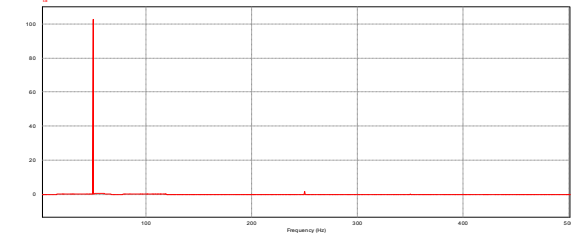


Figure 3.7 Simulation results of current  $i_{dc}$  and current  $i_q$  of fast charger model in inverter mode

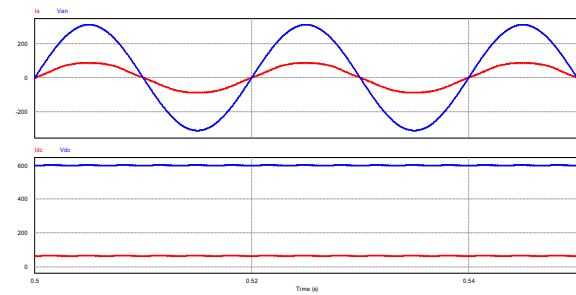
Modelling various levels of SOC are modelled with different levels of battery voltage level corresponding to the voltage drop of each battery cell. Voltage drop is greatest when the battery SOC is low, about 20%. Voltage drop on the battery with low SOC is around 77% of nominal battery voltage. Simulations performed with parameters of the battery voltage increased from 77%, 80%, 85%, and 90% of nominal voltage. Figure 3.8 - Figure 3.11 shows the results of simulation in a variety of battery voltage levels and their impacts on input current, source voltage.



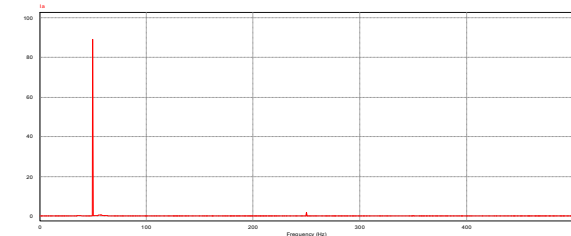
a. Input Voltage and Current (top), Output Voltage and Current (bottom)



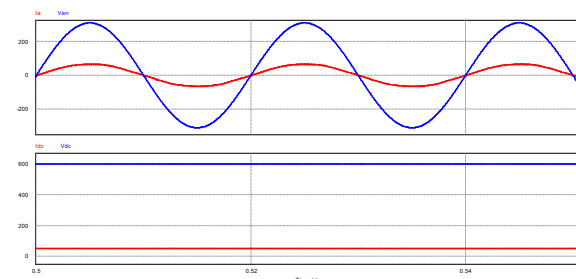
b. Harmonic Spectrum of Input Current  
Figure 3.8 Simulation results at 77% nominal voltage (462 V)



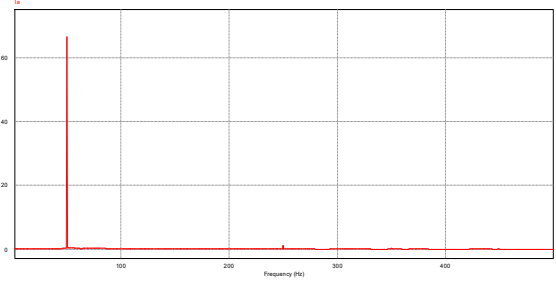
a. Input Voltage and Current (top), Output Voltage and Current (bottom)



b. Harmonic Spectrum of Input Current  
Figure 3.9 Simulation results at 80% nominal voltage (480 V)

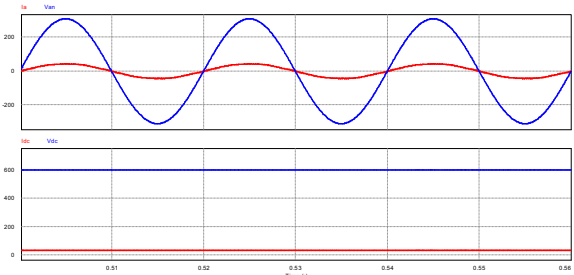


a. Input Voltage and Current (top), Output Voltage and Current (bottom)

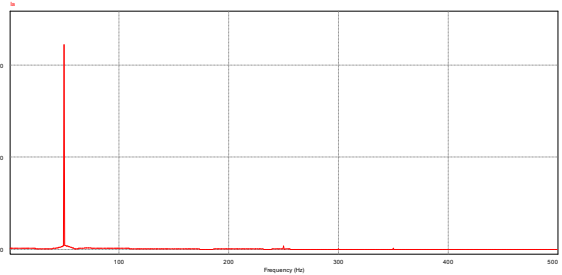


b. Harmonic Spectrum of Input Current

Figure 3.10 Simulation results at 85% nominal voltage (510 V)



a. Input Voltage and Current (top), Output Voltage and Current (bottom)



b. Harmonic Spectrum of Input Current

Figure 3.11 Simulation results at 90% nominal voltage (540V)

From the simulation results Figure 3.8 - Figure 3.11, it can be seen AC power input side and output side of the DC power from the circuit modelling of fast charging infrastructure with the following formula.

$$P_{ac} = \sqrt{3} \times V_{ll} \times I_L \quad (3.1)$$

$$P_{dc} = V_{dc} \times I_{dc} \quad (3.2)$$

Where  $V_{ll}$  is the voltage line-to-line rms source,  $I_L$  is the rms line current,  $V_{dc}$  is the average output, and  $I_{dc}$  is the average dc current flowing into the battery.

AC power input side and output side of the DC power when the battery voltage level range depends on the level of the battery SOC is like the data in Table 3.2. Evident from the simulation results that the lower the battery SOC value, the greater the power needed to charge the battery. SOC simulated battery voltage approaches the drop in battery cells. When the battery SOC 20% (77% nominal battery voltage) side of the DC power required to

charge the battery reaches about 45.92 kW, whereas when the SOC 80% (90% nominal battery voltage) power required in the DC is only about 18, 97 kW. This is appropriate because of the increase in SOC due to charging, the power needed to charge the batteries will be smaller.

TABLE 3.2 AC POWER INPUT AND DC POWER OUTPUT ON DIFFERENT SOC

Battery Voltage Level (% V nominal battery)	$V_{LL}$ (V)	$I_L$ (A)	$V_{dc}$ (V)	$I_{dc}$ (A)	$P_{ac}$ (W)	$P_{dc}$ (W)
462 V (77%)	380	72.7	599	76.5	47862	45923
480 V (80%)	380	63.0	596	63.0	41498	37622
510 V (85%)	380	53.4	597	48.5	35159	29017
540 V (90%)	380	31.6	599	31.6	20844	18976

Impact on the grid of fast charger is analyzed through simulation results of fast charging infrastructure model at various levels of SOC. Impact on the grid at different levels of SOC is seen from THD input current. THD at varying levels of SOC measured and simulated results are listed in Table 3.3. Judging from the results of measurements of THD simulation modelling of fast charging infrastructure, the input current THD tends to be greater at higher levels of SOC.

TABLE 3.3 THD FOR VARIOUS KIND OF BATTERY SOC

Battery Voltage Level	$I_L$ (A)	THD (%)
462 V (77% V nominal battery)	72.72	2.36
480 V (80% V nominal battery)	63.05	2.65
510 V (80% V nominal battery)	53.42	2.67
540 V (90% V nominal battery)	31.67	3.18

Through calculation, the input current THD can be determined by calculating the difference in  $I_L$  instantaneous value of rms current and fundamental rms current  $I_L$  defined as follows.

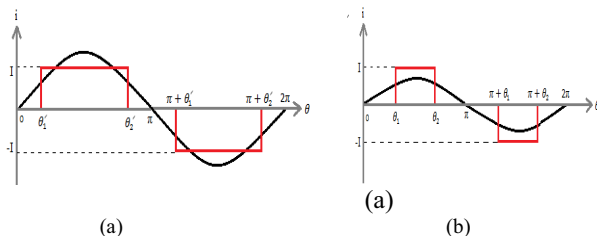


Figure 3.12 Instantaneous current  $i_L$  dan Fundamental Current  $I_L$  in different SOC (a) 20%, (b) 80%

$$THD = 100\% \times \frac{\sqrt{\left(\frac{1}{\pi} \int_{\theta_a}^{\theta_b} i_L dt\right)^2 - \left(\frac{1}{\pi} \int_{\theta_a}^{\theta_b} i_L \cos(\theta) dt\right)^2}}{\frac{1}{\pi} \int_{\theta_a}^{\theta_b} i_L \cos(\theta) dt} \quad (3.3)$$

When the battery SOC 20%, current that drawn from the source to charge the battery is large, with reference to Figure 3.12 assumed value  $\theta_1'$  and  $\theta_2' > \theta_1$  and  $\theta_2$  when the battery SOC 80%, then the THD of input current will be much smaller when the battery SOC 20% calculated from equation (3.3). Analysis of current THD calculation results is consistent with the results of simulation.

#### IV. CONCLUSION

Modelling of fast charging infrastructure as bidirectional three-phase PWM rectifier with dc output voltage control and current control input with simplified Lithium batteries models was successfully done using PSIM Simulation Software version 9.0.

Analysis results shows that a proposed current and voltage control method successfully maintained unity power factor and THD of input current below 5% on various SOC levels of the battery.

#### V. REFERENCE

- [1] S.Lacroix dan M. Hilariet, "An Integrated Fast Battery Charging for Electrical Vehicle", in Vehicle Power and Propulsion Conference (VPPC), September 2010.
- [2] J.V.F. Serra, "Electric Vehicles: Technology, Policy, and Commercial Development", Earthscan, 2012.
- [3] M. Yilmaz dan P. T. Kevin, "Review of Battery Charger Topologies, Charging Power Levels, and Infrastructure Plug-in Electric and Hybrid Vehicles", IEEE Transactions on Power Electronic Vol. 28 Hal 2151-2169, 2013.
- [4] S. Haghbin, dkk, "Integrated Charger for EV's and PHEV's : Examples and New Solutions", XIX International Convergence of Electrical Machine, 2010.
- [5] M. Grenier, M. g. Hossemi Aghdam, dan T. Thiringer, "Design On-Board Charger for Plug-in Hybrid Electrical Vehicle", in Vehicle Power and Propulsion Conference (VPPC), September 2011.
- [6] P.S. Moses, M.A.S. Masuum, dan S. Hajforoosh, "Overloading of Distribution Transformers in Smart Grid Due to Uncoordinated Charging of Plug-in Electric Vehicles", in Rec. IEEE PES Innovative Smart Grid Tech. Conf. (ISGT), January 2012.
- [7] J. Dannehl, C. Wessels, dan F. Wilhelm Fuch, "Limitations of Voltage-Oriented PI Current Control of Grid Connected PWM Rectifiers with LCL Filter", IEEE Transactions on Industrial Electronics, Vol.56 No 2, February 2009.
- [8] J. Dixon, "Three Phase Controlled Rectifier", Departement of Electrical Engineering, Pontificia Universidad Catolica de Chile.
- [9] [http://www.mynissanleaf.com/wiki/index.php?title=Battery\\_specs](http://www.mynissanleaf.com/wiki/index.php?title=Battery_specs), access on 11 March 2013 at 18.30.
- [10] Guozhen Hu, Shanxu Duan, Tao Cai, dan Baoqi Liu, "Modelling, Control, and Implementation of A Lithium-ion Battery Charger in Electric Vehicle Application", Przegląd Elektrotechniczny (Electrical Review) ISSN 0033-2097, R.88 NR 1b/2012.
- [11] F. Sasongko, "Sebuah Inverter Multilevel Modular Menggunakan Sumber Tegangan Searah Tunggal Sebagai Kompensator Daya Reaktif", Tesis, Program Studi Teknik Tenaga Listrik, Institut Teknologi Bandung, September 2011.
- [12] R. Teodorescu, M. Liserre, dan P. Rodriguez, "Grid Converters for Photovoltaic and Wind Power Systems", John Wiley & Sons, Ltd, 2011.
- [13] R. Wu, S.B. Dewan, G.R. Slemon, "A PWM AC to DC Converter with Fixed Switching Frequency", Industry Applications Society Annual Meeting, Conference Record on the 1988 IEEE Vol.1 Hal 706-711, 1988.
- [14] V. Blaskodan V. Kaura, "A New Mathematical Model and Control of Three-Phase AC-DC Voltage Source Converter", IEEE Transactions on Power Electronics Vol. 12 No.1, January 1997.7